Heliyon

Received:
30 November 2018
Revised:
29 January 2019
Accepted:
1 April 2019

Cite as:
Ateyyah M. AL-Baradi, Waleed A. Al-Shehri, Ali Badawi, Abdulraheem S. A. Almalki, Amar Merazga. A study of the nanostructure and efficiency of solid-state dye-sensitized solar cells based on a conducting polymer. Heliyon 5 (2019) e01472. doi: 10.1016/j.heliyon.2019.e01472

A study of the nanostructure and efficiency of solid-state dye-sensitized solar cells based on a conducting polymer

Ateyyah M. AL-Baradi [a,*], **Waleed A. Al-Shehri** [a], **Ali Badawi** [a], **Abdulraheem S. A. Almalki** [b], **Amar Merazga** [a]

[a] *Department of Physics, Faculty of Science, Taif University, Taif, 888, Saudi Arabia*

[b] *Department of Chemistry, Faculty of Science, Taif University, Taif, 888, Saudi Arabia*

[*] Corresponding author.

E-mail address: thobyani@yahoo.com (A.M. AL-Baradi).

Abstract

In this work the nanostructure and efficiency of solid-state dye-sensitized solar cells based on a conducting polymer have been investigated. A conducting polymer has been used as a solid-state electrolyte in the dye-sensitized solar cells. The polymer used in this study is a form of polythiophene synthesized in aqueous media. The obtained polymers were in two different structures: nanoparticles and networks. The structure of the synthesized polymers has been investigated using transmission electron microscope (TEM) and atomic force microscope (AFM). Furthermore, the optical and electrical properties of the synthesized polymers have also been considered. Solid-state dye-sensitized solar cells (SSDSCs) have been successfully constructed using these two polymers in addition to the linear poly(3-hexylthiophene) (P3HT). The photovoltaic characteristics of the assembled solar cells showed a good performance under annealing at 100 °C when using the network structure of polythiophene with a conversion power efficiency of 0.83%, while the nanoparticles polythiophene achieved 0.15% efficiency compared to 5.6×10^{-5}% when using P3HT.

Keywords: Materials science, Nanotechnology, Energy

https://doi.org/10.1016/j.heliyon.2019.e01472

1. Introduction

One of the leading research fields around the world is renewable energy. Solar cells in general are the best source of renewable energy because of their ability and sustainability. However, conventional solar cells with their high cost of production are not suitable for widespread applications. The past two decades has seen an increasing interest in replacing conventional solar cells with a low cost generation of solar cells. Liquid-electrolyte based dye-sensitized solar cells (DSCs) invented by Gratzel and co-workers in the 1991 are a promising generation that meets the requirements of clean and low cost renewable energy sources [1, 2, 3]. DSCs consist of films of porous metal oxide nanoparticles such as ZnO and TiO_2, and are classified as a third generation of solar cells [4, 5, 6, 7]. One of the drawbacks of DSCs based on liquid electrolytes is the leakage and vaporization of the solvent, which limits the durability and stability of the cells. Therefore, the solidification of the electrolyte in DSCs has been one of the most important routes to overcome this problem [8, 9]. A lot of research has been conducted to replace the liquid electrolyte with solid or gel materials [10, 11, 12, 13, 14]. Hole transporting materials (HTM) are usually utilized as solid-state electrolytes in DSCs including inorganic types such as CuI and CuSCN, and organic types such as Spiro-OMeTAD [15, 16]. However, because of their low conversion efficiency due to poor penetration into the nanoporous film, they cannot satisfy the requirements of DSCs application [17]. Nanofiber membranes have been utilized as quasi-solid state electrolytes in DSCs showing an acceptable performance [18]. Another problem facing DSCs is the interactions between the electrolyte and TiO_2, which can be overcome by using polymers with hydrophobic groups [19]. Polymer gel electrolytes have also attracted attention in DSCs and the most frequently used polymers are poly(ethylene oxide) (PEO), poly(methyl methacrylate) (PMMA) and polyvinyl alcohol (PVA) [20, 21]. Due to their instability, these polymers face some serious challenges such as iodine crystallization, phase separation, and the strict sealing procedure required to produce DSCs with best durability and stability [22]. Conducting polymers have been tried for hole-transporting materials in DSCs. Wagner et al. described the use of carbazole-based polymers in DSCs with hole-conducting polymer [23]. Kudo et al. fabricated the organic-inorganic hybrid solar cells based on a conducting polymer and SnO_2 nanoparticles [24]. Polyaniline (PANI) is known as a wide band-gap HTM. Ameen et al. have reported the application of PANI in DSC photo-electrode using N710 and Z907 as sensitizers [25]. Polythiophene and its derivatives have been utilized in many fields such as, electrolytes and flexible devices [26, 27]. As an example, polythiophene with different structures has been applied in SSDSCs

https://doi.org/10.1016/j.heliyon.2019.e01472

as hole transporting media [28, 29, 30, 31, 32]. These electrolytes showed acceptable efficiency and stability [33, 34].

In this work, polythiophene synthesized in aqueous medium with different structures will be used as a hole-transporting material in DSCs. The morphological effect of this polymer on the TiO_2 will be investigated using AFM. The optical properties of such polymer will be explored. Moreover, the photovoltaic characteristics of the obtained SSDSCs will be studied by recording the following parameters: short circuit current density (Jsc), open circuit voltage (Voc), fill factor (FF) and energy conversion efficiency (η).

2. Experimental

Polythiophene was synthesized by mixing cetyltrimenthylammon-ium bromide (CTAB, 0.82 g), triethanolamine (TEA, 2.6 g) and thiophene (1.25 mL) with deionized water (15 mL) in a bottom-rounded flask. The mixture was sonicated for 30 min. Ammonium persulfate (APS 4.31 g) was dissolved in 10 mL of deionized water and added dropwise to the first mixture mentioned above. The final mixture was then heated without stirring at 70 °C for 24 h. The polymer samples through this reaction showed a controlled morphology between spherical particles and fibers (network) by changing the ratio of TEA from 2.6 g to 6.5 g, respectively. Fig. 1 shows TEM images of particle and network nanostructures.

The photo-electrode of SSDSCs was prepared using TiO_2 coated TCO as received from Solaronix dipped into ruthenium-based dye ($C_{26}H_{20}O_{10}$-N_6S_2Ru), known as N3 for 6 hours. The dye solution was prepared by dissolving 2 mg of N3 into 10 ml of ethanol. The dyed TiO_2 electrodes were then washed with acetonitrile and the obtained photo-electrodes were coated with polythiophenes using spin coating at speed of 3000 rpm for 30 s. These films were studied as prepared and with annealing at 100 °C. The surface morphology of the prepared photoelectrodes was studied

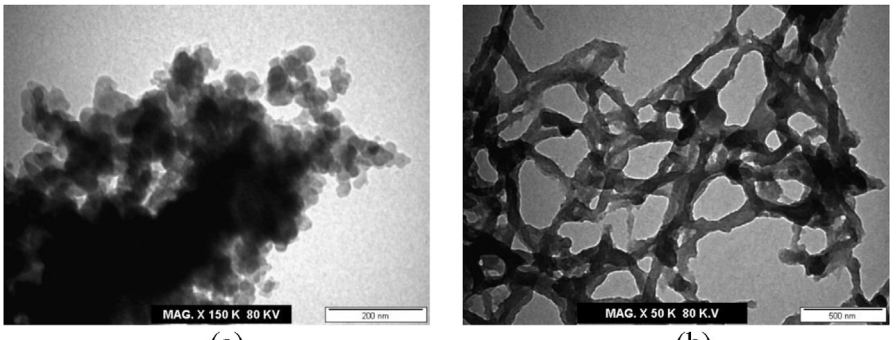

Fig. 1. TEM images of polythiophene with different structures; (a) PTh nanoparticles and (b) PTh network structures.

https://doi.org/10.1016/j.heliyon.2019.e01472

using a Dimension 3100 AFM with Nanoscope IV controller (Veeco Instruments). A silicon tip with <10 nm tip radius, typical spring constant 40 N/m and resonant frequency of ≈ 300 kHz was used for imaging in Tapping mode under ambient conditions. A UV−vis spectrophotometer (Jasco V-570) was utilized to measure the absorbance of the polythiophene solutions and N3 dye.

Three cells of each type of SSDSCs were constructed by assembling the prepared photo-electrodes against FTO-glass substrate coated with platinum catalyst (Solaronix) using paper clips. A 0.25 cm^2 illuminated area was made on the glass substrate by using a mask from black tape. A photovoltaic system consisting of a solar simulator (Solar-Light) and an electrometer (Keithley 2400) was utilized to obtain the I−V characteristics of the prepared SSDSCs. The system is computer-controlled to acquire and plot the I−V data after AM1.5-filtered light from the 300 WXenon lamp of the solar simulator shines the SSDSC at a power density $P_i = 100$ mW/cm^2. Each measurement was repeated three times and the errors in the efficiency were then calculated. The photovoltage V_{oc} decay from steady state over a time range of 10 s was measured by a Tektronix 500 MHz oscilloscope to test the recombination rate in SSDSCs.

3. Results & discussion

The three different polythiophene structures were spin-coated onto a silicon substrate to measure the expected film thickness of each polymer using an ellipsometer. The thicknesses of the obtained films were ranging from almost 24 nm−34 nm as shown in Table 1. These polymers were also spin-coated onto prepared photoelectrodes and the AFM was used to study the interface between these layers. Fig. 2 (top left) shows an AFM image of TiO_2 photoelectrode as prepared without any coating. It can be seen from this figure the nanoparticles of TiO_2 have well defined structures with an average size around 20 nm in diameter. The average roughness in this case (the RMS value) is almost 30 nm (see Table 1). In comparison, Fig. 2 (top right)

Table 1. The roughness at room temperature and 100 °C and the thickness of coated and un-coated TiO_2 measured by AFM and Ellipsometry.

Film structure	Roughness by AFM (RMS) @ 25 °C (nm)	Roughness by AFM (RMS) @ 100 °C (nm)	Thickness (by Ellipsometer) (nm)
TiO_2 without coating	30.0	30.0	N/A
TiO_2 + P3HT	27.7	32.6	34.6
TiO_2 + polythiophene network	28.0	14.3	27.5
TiO_2 + polythiophene nanoparticles	24.2	17.1	24.4

https://doi.org/10.1016/j.heliyon.2019.e01472

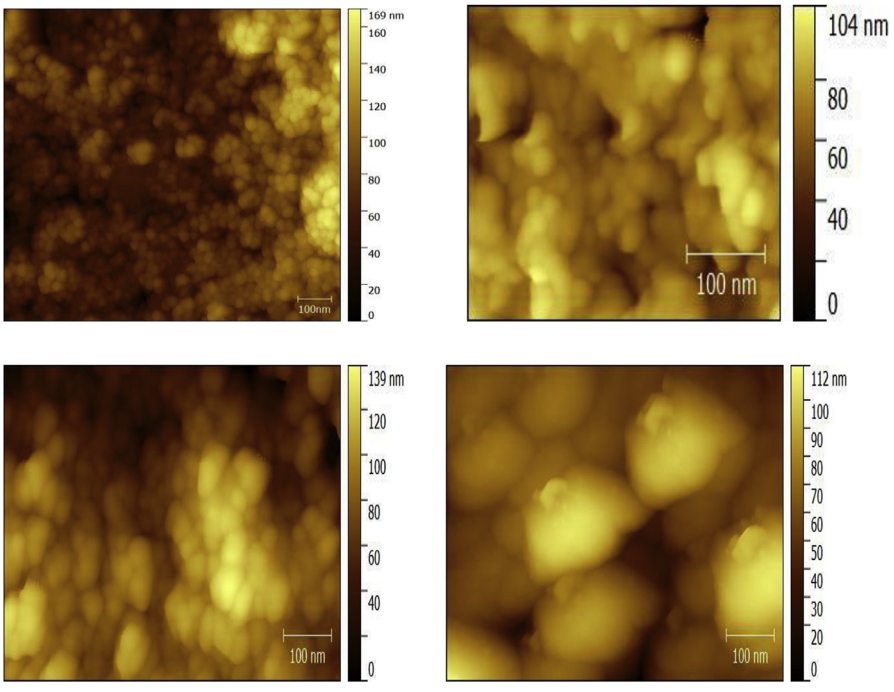

Fig. 2. AFM images of uncoated TiO_2 photoelectrode (top left) and coated TiO_2 photoelectrode with P3HT (top right), polythiophene network (bottom left) and polythiophene nanoparticles (bottom right) at room temperature.

shows a coated TiO_2 photoelectrode with P3HT. It is clear from this figure that the morphology of the film has changed and this can be attributed to P3HT single molecules being penetrated and filled the pores of TiO_2 layer. When the layer of TiO_2 is coated with P3HT, the roughness decreases to 27 nm (Table 1). Fig. 2 (bottom left) shows the coated TiO_2 photoelectrode with a network-structured polythiophene. The figure shows that the morphology of the film does not change significantly compared to the P3HT case. The reason behind this is that the mesh size of the polymer network is definitely larger than the TiO_2 particle size (shown in SEM images in Fig. 1 (a)). This results in TiO_2 particles penetrating the polymer network having well defined particle structures on the surface. The increase of the particle size at the surface due to the polymer network coating is also noticeable in Fig. 2 (bottom left). The roughness in this case is similar to that in the case of P3HT (27 nm). Fig. 2 (bottom right) shows the coating of TiO_2 with a nanoparticle-structured polythiophene. This figure shows different morphology from the two structures mentioned above. The grain size shown in Fig. 2 (bottom right) has increased many times compared to the other two cases. This can be explained due to the aggregation of polythiophene nanoparticles around TiO_2 particles at the surface. This aggregation at the surface happens because of the large size of polythiophene nanoparticles which cannot penetrate the pours of TiO_2 as shown in SEM images in Fig. 1(b). The roughness of the film slightly decreases in this case to 24 nm compared to 27 nm and 28 nm in the case of P3HT and polythiophene network, respectively. It

https://doi.org/10.1016/j.heliyon.2019.e01472

can be concluded that the surface of TiO_2 can be manipulated using different structures of polythiophenes, which results in different morphologies.

It is known that polymer structures are affected by temperature variation, especially near the glass transition temperature (T_g) of the polymer. The morphology of the polymers mentioned above on the top of TiO_2 has been investigated at 100 °C. Previous studies also found that the peak absorption wavelength λ_{max} for the untreated film of similar polymers to this study is 495 nm and 515 nm at room temperature and 110 °C, respectively [29]. It was also found that heating the samples at temperatures higher than 110 °C shows similar behavior of the absorption spectra. Fig. 3 shows the change of morphology with increasing temperature for all structures of polythiophene. In the case of P3HT (Fig. 3 left), TiO_2 nanoparticles have well defined shapes similar to that at room temperature shown in Fig. 2 (top right). The reason behind this is that P3HT molecules have diffused through TiO_2 pores with increasing temperature. This is confirmed by the change in roughness from 27.7 nm to 32.6 nm as shown in (Table 1). In the case of polythiophene network (Fig. 3, middle), the polymer surface shows smoothness more than that at room temperature with a decrease in the roughness from 28.0 nm to 14.3 nm as shown in (Table 1). Similarly, the nanoparticle-structured polythiophene (Fig. 3, right) has the same effect with temperature showing a decrease in the roughness from 24.2 nm to 17.1 nm.

It is worthwhile studying the optical behavior of the synthesized polymers compared to that of the dye used in the dye-sensitized solar cells. Fig. 4 shows the absorption spectra of N3 and the different structures of polythiophene. It is clear from this figure that P3HT has a very low absorption with a similar absorption edge to nanoparticle and network structures. A similar behavior was observed in the case of polythiophene nanoparticles with a similar absorption as P3HT. On the other hand, polythiophene network has an absorption peak at around 550 nm with a similar behavior to the N3 dye. This means that polythiophene networks have the ability to absorb visible light, which can contribute positively in the SSDSCs. From Fig. 4 it is clear that N3 dye and polythiophene network have the same absorption edges, although the absorption intensity is

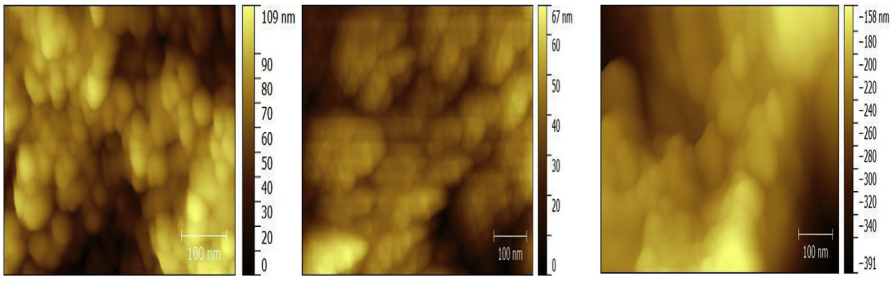

Fig. 3. AFM images of coated TiO_2 photoelectrodes with P3HT (left), polythiophene network (middle) and polythiophene nanoparticles (right) at 100 °C.

https://doi.org/10.1016/j.heliyon.2019.e01472

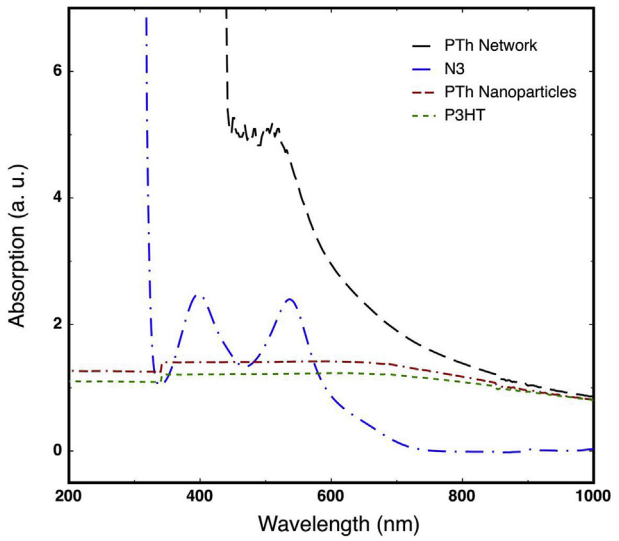

Fig. 4. Absorption spectra of N3-dye and different structures of polythiophene.

higher in the case of polythiophen network. This might indicate a larger band-gap in polythiophene network compared to the N3 dye.

SSDSCs were constructed using different polythiophene structures. The results obtained from the SSDSCs will be compared with conventional DSCs based on liquid electrolyte. During the cell preparation, the TiO_2 layer must be covered with the dye. Dying time has been found to affect the performance of the solar cells. Therefore, an optimization has to be done to choose the optimal time for dying the TiO_2 layer. Three different dying times were tested (2, 6 and 9 h) and the best dying time was found to be 6 h and this dipping time has been used throughout this study.

Fig. 5 shows the I-V characteristic curves of the solid-state dye-sensitized solar cells based on different structures of polythiophene. This figure shows that the cell based on polythiophene network structure gives the optimal photovoltaic performance with power conversion efficiency (η) of 0.005% corresponding to a photocurrent of 0.035 mA. However, this performance considerably decreases when the nanoparticle of polythiophene or P3HT are used. On the other hand, Fig. 6 shows the I-V curves of the same samples after annealing at 100 °C. The performance of the cells was improved by more than two orders of magnitude as shown (Table 2). The reason behind this increase in efficiency after annealing is the change of the polymer morphology where the AFM images showed that the interface between polythiophene networks and TiO_2 has a similar morphology to that of un-coated photoelectrode. This means that the network layer does not affect the function of TiO_2 nanoparticles in the cell. This result indicates that polythiophene networks are good candidates for solid-state DSCs especially when they are annealed up to

https://doi.org/10.1016/j.heliyon.2019.e01472

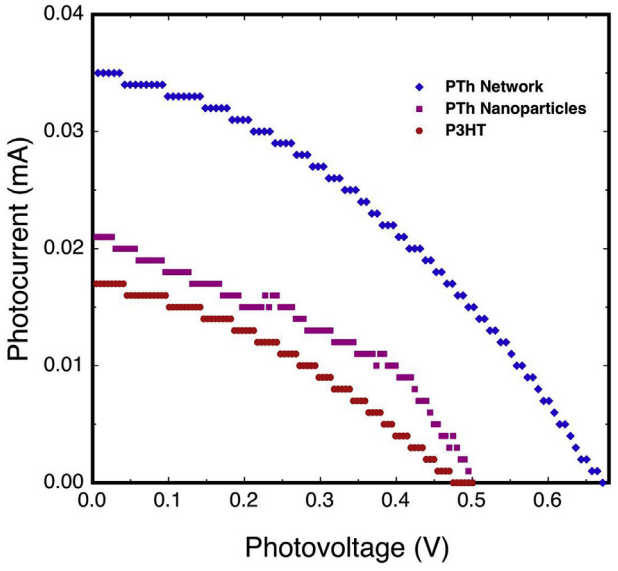

Fig. 5. I-V characteristics of a SSDSC using three different structures of polythiophene at room temperature.

100 °C. The obtained power conversion efficiency (η) from the cell containing poythiophene networks is 0.83% corresponding to a photocurrent of 0.65 mA, which is comparable to that of DSCs based on liquid electrolyte with power conversion efficiency of 1.24 corresponding to a photocurrent of 0.99 mA (see Table 2). While, a slight increase in the performance of the solar cell upon heating has been observed in the case of P3HT and nanoparticle-structured polythiophene as shown in Fig. 6 and Table 2. Furthermore, the increase in power conversion efficiency in the case of the network structure is attributed to the increase in optical absorption of polythiophene

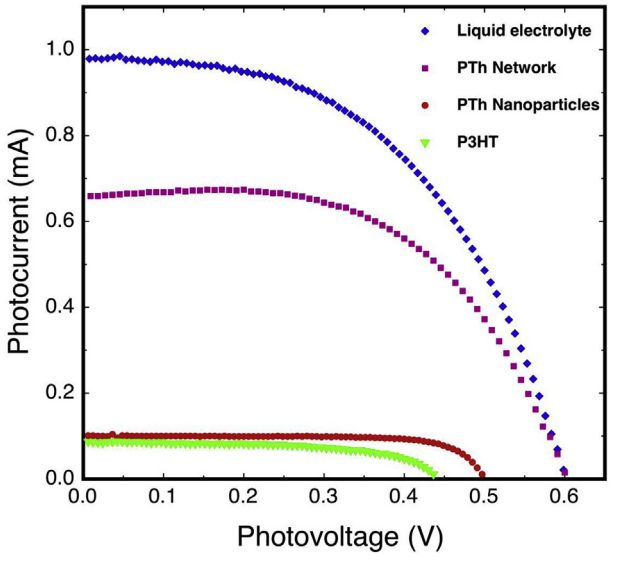

Fig. 6. I-V characteristic curves of a SSDSC using three different structures of polythiophene at 100 °C.

https://doi.org/10.1016/j.heliyon.2019.e01472

Table 2. Photovoltaic parameters obtained from DSCs and SSDSCs at room temperature and 100 °C. Note: conventional DSC with liquid electrolyte was not heated.

Sample	I_{sc} (mA)		J_{sc} (mA/cm^2)		V_{oc} (V)		FF		η (%)		R_s (Ω)
	Room Temp.	100 °C	Room Temp.	100 °C	Room Temp.	100 °C	Room Temp.	100 °C	Room Temp.	100 °C	100 °C
P3HT	0.017	0.09	0.06	0.32	0.49	0.44	0.25	0.28	$7.3 \times 10^{-5} \pm 1.5 \times 10^{-6}$	$5.6 \times 10^{-5} \pm 3.1 \times 10^{-6}$	132
Nanoparticles	0.021	0.10	0.07	0.35	0.50	0.50	0.26	0.30	$9.1 \times 10^{-4} \pm 7 \times 10^{-5}$	0.15 ± 0.01	88
Network	0.035	0.63	0.12	2.23	0.68	0.6	0.61	0.68	$5 \times 10^{-3} \pm 1 \times 10^{-3}$	0.83 ± 0.05	40
Liquid electrolyte	0.99	------	4.5	------	0.6	-----	0.45	-----	1.24 ± 0.15	-----	35

https://doi.org/10.1016/j.heliyon.2019.e01472

networks compared to the other polythiophene structures. This increase in absorption assists the dye to compensate the lost electrons through the transportation of the hole and also inject electrons from the LUMO of the polymer directly to conduction band of TiO_2. The low value of the fill factor can be attributed to the increase of the series resistance (R_s) as shown in Table 2. In addition, the high values of R_s in the case of P3HT and PTh nanoparticles led to the decease in the photocurrent (I_{sc}).

The dark I-V characteristics have been found to give some interpretation of the enhancement of DSCs efficiency in terms of the energy barrier caused by the coating on the photoelectrode. Fig. 7 shows the dark I-V characteristic curves of a conventional DSC and SSDSCs using different structures of polythiophene. In the dark, electron injection from the dye is absent and the current is only generated by the diffusion of electrons from TiO_2 semiconductor to the electrolyte in DSC and the polymer in SDSCs [28]. It is clear from Fig. 7 that, when adding the polymer layer, the energy barrier increases as indicated by the increase in the voltage because electrons in this case require a higher voltage to overcome the barrier. The situation became worse when using the nanoparticle-structured polythiophene and P3HT.

Furthermore, V_{oc}−decay from steady state is another tool to investigate the back-transport and recombination behavior in DSCs. Fig. 8 shows V_{oc}−decay curves for SSDSCs based on different polythiophene structures. It is clear from this figure that the V_{oc}−decay is much slower in the case of the network structure followed by the nanoparticle structure and finally the linear structure of polythiophene. Since the rate of V_{oc}− decay is proportional to the recombination rate, it is evident that the rate of combination decreases when using the network structure of polythiophene

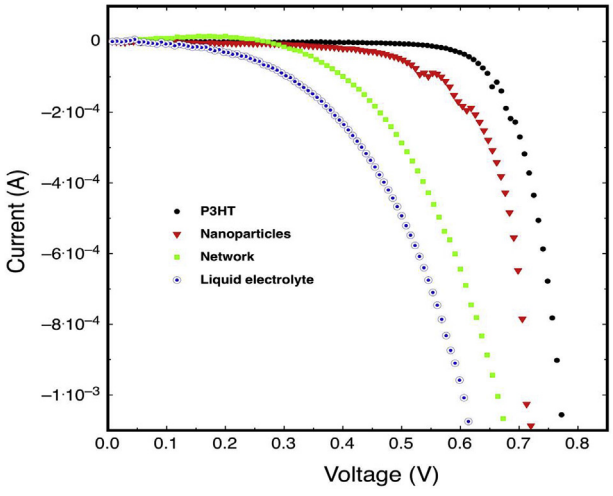

Fig. 7. Dark I-V characteristics of different DSCs using liquid electrolyte and different polythiophene structures.

https://doi.org/10.1016/j.heliyon.2019.e01472

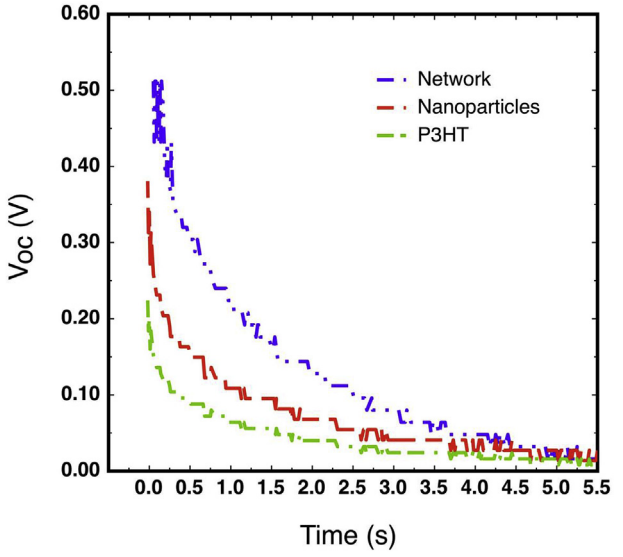

Fig. 8. V_{oc} decay following suppression of illumination for SDSCs using different polythiophene structures.

because it is a good hole transporting material, which led to the increase in (η) seen above.

4. Conclusion

Solid-state dye-sensitized solar cells were successfully constructed using different structures of polythiophene as hole-transporting media in comparison to conventional dye-sensitized solar cells based on liquid electrolyte. This study showed that the network-structured polythiophene is a good candidate as a hole-transporting medium giving an efficiency of 0.83% with annealing at 100 °C, which is comparable to 1.24% obtained from a conventional DSC. The structural and morphological study by SEM and AFM in addition to the optical investigation gave a good interpretation for the increase of the efficiency in the case of the network-structured polythiophene compared to the nanoparticle-structured polythiophene and P3HT.

Declarations

Author contribution statement

Ateyyah M. Al-Baradi: Conceived and designed the experiments; Wrotethe paper.

Waleed A. Al-Shehri:Performed the experiments.

Ali Badawi, Abdulraheem S. A. Almalki, Amar Merazega: Analyzed and interpreted the data; Wrote the paper.

https://doi.org/10.1016/j.heliyon.2019.e01472

Funding statement

This work was supported by Taif University (project No. 1-435-3653) and King Abdulaziz City for Science and Technology.

Competing interest statement

The authors declare no conflict of interest.

Additional information

No additional information is available for this paper.

References

[1] B. O'regan, G. Michael, A low-cost, high-efficiency solar cell based on dye-sensitized colloidal TiO2 films, Nature 353 (1991) 737.

[2] M. Grätzel, Dye-sensitized solid-state heterojunction solar cells, MRS Bull. 30 (2005) 23−27.

[3] M. Grätzel, The light and shade of perovskite solar cells, Nat. Mater. 13 (2014) 838.

[4] A. Hagfeldt, V. Nikolaos, Dye-sensitized solar cells, in: The Future of Semiconductor Oxides in Next-Generation Solar Cells, 2018, pp. 183−239.

[5] M. Law, E.G. Lori, C.J. Justin, S. Richard, Y. Peidong, Nanowire dye-sensitized solar cells, Nat. Mater. 4 (2005) 455.

[6] M. Freitag, T. Joël, S. Yasemin, Z. Xiaoyu, G. Fabrizio, L. Paul, H. Jianli, et al., Dye-sensitized solar cells for efficient power generation under ambient lighting, Nat. Photon. 11 (2017) 372.

[7] J. Gong, K. Sumathy, Q. Qiquan, Z. Zhengping, Review on dye-sensitized solar cells (DSCs): advanced techniques and research trends, Renew. Sustain. Energy Rev. 68 (2017) 234−246.

[8] Y. Cao, S. Yasemin, U. Amita, T. Joël, L. Jingshan, P. Norman, G. Fabrizio, et al., 11% efficiency solid-state dye-sensitized solar cells with copper (II/I) hole transport materials, Nat. Commun. 8 (2017) 15390.

[9] J. Zhang, F. Marina, H. Anders, B. Gerrit, Solid-state dye-sensitized solar cells, in: Molecular Devices for Solar Energy Conversion and Storage, 2018, pp. 151−185.

https://doi.org/10.1016/j.heliyon.2019.e01472

[10] U. Bach, D. Lupo, P. Comte, J.E. Moser, F. Weissörtel, J. Salbeck, H. Spreitzer, M. Grätzel, Solid-state dye-sensitized mesoporous TiO_2 solar cells with high photon-to-electron conversion efficiencies, Nature 395 (1998) 583.

[11] H.A. Al-Mohsin, Kenneth P. Mineart, D.P. Armstrong, A. El-Shafei, R.J. Spontak, Quasi-solid-state dye-sensitized solar cells containing a charged thermoplastic elastomeric gel electrolyte and hydrophilic/phobic photosensitizers, Solar RRL 2 (2018) 1700145.

[12] A. Delices, Z. Jinbao, S. Marie-Pierre, D. Chang-Zhi, M. Francois, V. Nick, H. Anders, J. Mohamed, New covalently bonded dye/hole transporting material for better charge transfer in solid-state dye-sensitized solar cells, Electrochim. Acta 269 (2018) 163−171.

[13] P. Qin, S. Paek, M.I.D., R. Kasparas, E. Hany, S.A. Al-Muhtaseb, L. Christian, K.N. Mohammad, Weakly conjugated hybrid zinc porphyrin sensitizers for solid-state dye-sensitized solar cells, Adv. Funct. Mater. 26 (2016) 5550−5559.

[14] P. Docampo, G. Stefan, L. Tomas, K.N. Nakita, S. Ullrich, J.S. Henry, Lessons learned: from dye-sensitized solar cells to all-solid-state hybrid devices, Adv. Mater. 26 (2014) 4013−4030.

[15] X. Chen, L. Qing, Z. Jie, Q. Lihua, Z. Yueguang, S. Baoquan, Y. Feng, Ionic liquid-tethered nanoparticle/poly (ionic liquid) electrolytes for quasi-solid-state dye-sensitized solar cells, J. Power Sources 207 (2012) 216−221.

[16] N.S. Sariciftci, S. Sam-Shajing (Eds.), Organic Photovoltaics: Mechanism, Materials, and Devices, Taylor & Francis, New York, 2005.

[17] B. Xu, B. Dongqin, H. Yong, L. Peng, C. Ming, M. Grätzel, K. Lars, H. Anders, S. Licheng, A low-cost spiro [fluorene-9, 9′-xanthene]-based hole transport material for highly efficient solid-state dye-sensitized solar cells and perovskite solar cells, Energy Environ. Sci. 9 (2016) 873−877.

[18] M.P. Balanay, R. Nirmala, D.H. Kim, N. Senthilkumar, A.R. Kim, D.J. Yoo, The photovoltaic performances of PVdF-HFP electrospun membranes employed quasi-solid-state dye sensitized solar cells, J. Nanosci. Nanotechnol. 16 (2016) 581−587.

[19] D.J. Yoo, A.R. Kim, M.P. Balanay, D.H. Kim, Alkoxy-substituted triphenylamine based chromophores for dye-sensitized solar cells, Bull. Korean Chem. Soc. 33 (2012) 33−34.

https://doi.org/10.1016/j.heliyon.2019.e01472

[20] Y. Yang, C.H. Zhou, S. Xu, H. Hu, B.L. Chen, J. Zhang, et al., Improved stability of quasi-solid-state dye-sensitized solar cell based on poly (ethylene oxide)−poly (vinylidene fluoride) polymer-blend electrolytes, J. Power Sources 185 (2008) 1492−1498.

[21] H.W. Han, W. Liu, J. Zhang, X.Z. Zhao, A hybrid poly (ethylene oxide)/poly (vinylidene fluoride)/TiO2 nanoparticle solid-state redox electrolyte for dye-sensitized nanocrystalline solar cells, Adv. Funct. Mater. 15 (2005) 1940−1944.

[22] X. Chen, Q. Li, J. Zhao, L. Qiu, Y. Zhang, B. Sun, F. Yan, Ionic liquid-tethered nanoparticle/poly (ionic liquid) electrolytes for quasi-solid-state dye-sensitized solar cells, J. Power Sources 207 (2012) 216−221.

[23] J. Wagner, J. Pielichowski, A. Hinsch, K. Pielichowski, D. Bogdał, M. Pajda, et al., New carbazole-based polymers for dye solar cells with hole-conducting polymer, Synth. Met. 146 (2004) 159−165.

[24] N. Kudo, Y. Shimazaki, H. Ohkita, M. Ohoka, S. Ito, Organic−inorganic hybrid solar cells based on conducting polymer and SnO_2 nanoparticles chemically modified with a fullerene derivative, Sol. Energy Mater. Sol. Cells 91 (2007) 1243−1247.

[25] S. Ameen, M.S. Akhtar, Y.S. Kim, O.B. Yang, H.S. Shin, Sulfamic acid-doped polyaniline nanofibers thin film-based counter electrode: application in dye-sensitized solar cells, J. Phys. Chem. C 114 (2010) 4760−4764.

[26] J. Zhang, N. Vlachopoulos, M. Jouini, M.B. Johansson, X. Zhang, M.K. Nazeeruddin, A. Hagfeldt, Efficient solid-state dye sensitized solar cells: the influence of dye molecular structures for the in-situ photoelectrochemically polymerized PEDOT as hole transporting material, Nano Energy 19 (2016) 455−470.

[27] Y. Yu, M. Lira-Cantu, Solid state dye sensitized solar cells applying conducting organic polymers as hole conductors, Phys. Proc. 8 (2010) 22−27.

[28] M. Chevrier, H. Hawashin, S. Richeter, A. Mehdi, M. Surin, R. Lazzaroni, S. Clément, Well-designed poly (3-hexylthiophene) as hole transporting material: a new opportunity for solid-state dye-sensitized solar cells, Synth. Met. 226 (2017) 157−163.

[29] G. Li, V. Shrotriya, Y. Yao, Y. Yang, Investigation of annealing effects and film thickness dependence of polymer solar cells based on poly (3-hexylthiophene), J. Appl. Phys. 98 (2005) 043704.

 https://doi.org/10.1016/j.heliyon.2019.e01472

[30] J. Halme, Dye-sensitized Nanostructured and Organic Photovoltaic Cells: Technical Review and Preliminary Tests, 2002.

[31] C.Y. Tan, F.S. Omar, N.M. Saidi, N.K. Farhana, S. Ramesh, K. Ramesh, Optimization of poly (vinyl alcohol-co-ethylene)-based gel polymer electrolyte containing nickel phosphate nanoparticles for dye-sensitized solar cell application, Sol. Energy 178 (2019) 231−240.

[32] F. Bella, J. Popovic, A. Lamberti, E. Tresso, C. Gerbaldi, J. Maier, Interfacial effects in solid−liquid electrolytes for improved stability and performance of dye-sensitized solar cells, ACS Appl. Mater. Interfaces 9 (2017) 37797−37803.

[33] A. Scalia, F. Bella, A. Lamberti, C. Gerbaldi, E. Tresso, Innovative multipolymer electrolyte membrane designed by oxygen inhibited UV-crosslinking enables solid-state in plane integration of energy conversion and storage devices, Energy 166 (2019) 789−795.

[34] F. Bella, A. Sacco, G. Massaglia, A. Chiodoni, C.F. Pirri, M. Quaglio, Dispelling clichés at the nanoscale: the true effect of polymer electrolytes on the performance of dye-sensitized solar cells, Nanoscale 7 (2015) 12010−12017.

https://doi.org/10.1016/j.heliyon.2019.e01472